https://doi.org/10.5194/esd-2022-53
Preprint. Discussion started: 15 December 2022

Earth System Dynamics Discussions
Open Access
EGU

Groundwater in terrestrial systems modelling: a new climatology of extreme heat events in Europe

Liubov Poshyvailo-Strube[1,2], Niklas Wagner[1,2], Klaus Goergen[1,2], Carina Furusho-Percot[3], Carl Hartick[1,2], and Stefan Kollet[1,2]

[1]Institute of Bio- and Geosciences: Agrosphere (IBG-3), Forschungszentrum Jülich, Jülich, Germany
[2]Centre for High-Performance Scientific Computing in Terrestrial Systems (HPSC TerrSys), Geoverbund ABC/J, Jülich, Germany
[3]National Research Institute for Agriculture, Food and the Environment (INRAE), Avignon, France

Correspondence: Liubov Poshyvailo-Strube (l.poshyvailo@fz-juelich.de)

Abstract. Due to climate change, years with positive temperature anomalies are becoming more frequent in Europe, requiring high-resolution climate data to plan for climate change mitigation and adaptation. However, many regional climate models (RCMs) simplify the representation of groundwater processes, leading to biases in simulated extreme heat events. Here, we study the characteristics of summer heat events in a unique dataset from the regional Terrestrial Systems Modeling Platform (TSMP) simulations, compared to an ensemble of EURO-CORDEX climate change scenario control simulations, for the historical time period 1976-2005.

Our results show that in TSMP, the impact of groundwater coupling on the frequency of hot summer days depends on the considered time period and the region, associated with respective evaporative regime. An increasing trend of the frequency of hot summer days averaged across Europe is the lowest in TSMP compared to the other RCMs considered. Groundwater coupling has a systematic effect on the duration and intensity of heat events: summer heat events with long duration and high intensity are less frequent in TSMP compared to the CORDEX ensemble. In particular, extended heat events with a duration exceeding 6 days, i.e. heat waves, occur on average in Europe about 1.5-8 times less often in TSMP, while single-day heat events happen slightly more often in TSMP compared to the CORDEX ensemble. The frequency of high-intensity heat waves in TSMP is up to 12 times lower on average in Europe compared to the CORDEX ensemble. Thus, an explicit groundwater representation in RCMs may lead to rarer and weaker heat waves in Europe also in climate projections. The findings of this work indicate an existing discrepancy in the ensemble of EURO-CORDEX climate change scenario control simulations and emphasize the importance of groundwater representation in RCMs.

1 Introduction

The number of extreme heat events has increased in recent decades (e.g., Frich et al., 2002; Alexander et al., 2006; Christidis et al., 2015; Zhang et al., 2020). Especially, 2003, 2010, and 2018 were exceptionally hot years in Europe, characterised by record-breaking air temperatures (e.g., Stott et al., 2004; Barriopedro et al., 2011; Liu et al., 2020; Dirmeyer et al., 2021). With projected climate change, the frequency of such extreme events will increase (e.g., Russo et al., 2015; Myhre et al., 2019; Hari

https://doi.org/10.5194/esd-2022-53
Preprint. Discussion started: 15 December 2022


Earth System Dynamics Discussions

et al., 2020; Molina et al., 2020; Masson-Delmotte et al., 2021), leading to multiple negative socio-economic impacts (e.g., Bosello et al., 2007; Ciscar et al., 2011; Amengual et al., 2014; Naumann et al., 2021).

The underlying hydrometeorological mechanisms of heat events have been extensively studied (e.g., Lhotka and Kyselý, 2015; Horton et al., 2016; Lhotka et al., 2018; Liu et al., 2020). The evolution of extreme heat events or heat waves depends primarily on the synoptic weather patterns in combination with ambient soil moisture conditions, further altered by multiple land-atmosphere feedback processes (e.g., Fischer et al., 2007; Horton et al., 2016). Heat waves are triggered by strong, persistent quasi-stationary large-scale high pressure systems with subsiding, warming air masses and atmospheric blocking events, as well as clear skies that enable a high amount of solar radiation (Tomczyk and Bednorz, 2016; Horton et al., 2016). Moreover, atmospheric blocking events impact winter/early spring precipitation over most of Europe, affecting soil moisture (e.g., Vautard et al., 2007; Ionita et al., 2020).

Many European summer heat waves were preceded by a deficiency of spring precipitation (Dirmeyer et al., 2021; Stegehuis et al., 2021; Hartick et al., 2021). The effect of soil moisture memory, associated with long-term (from weeks to months) persistence of wet or dry anomalies, allows to preserve the hydroclimatic conditions of preceding months (Martínez-de la Torre and Miguez-Macho, 2019; Song et al., 2019). Thus, the lack of precipitation in early spring causes negative soil moisture anomalies in early summer, and leads to a stronger moisture-limited land-atmosphere coupling (a measure of response of the atmosphere to anomalies in the land surface state) with a lower evaporation fraction. As a result, latent cooling decreases and amplifies summer temperatures (e.g., Fischer et al., 2007; Miralles et al., 2012; Erdenebat and Tomonori, 2018; Dirmeyer et al., 2021). Apart from precipitation, soil moisture content and distribution are strongly affected by subsurface hydrodynamics through vertical and lateral fluxes that connect groundwater with the land surface. In this connection, the water table depth influences the intensity of groundwater–soil moisture and soil moisture-temperature coupling (Barlage et al., 2015; Keune et al., 2016; Mu et al., 2021).

In the context of e.g. climate change impact studies, dynamical downscaling of global climate models (GCMs) with regional climate models (RCMs) provides the required high-resolution climate information (Taylor et al., 2012; Mearns et al., 2015; Gutowski et al., 2020). Most of the multi-model RCM ensemble simulations performed over Europe follow the common protocol of the Coordinated Regional Climate Downscaling Experiment for European domain (EURO-CORDEX) (e.g., Gutowski et al., 2016; Jacob et al., 2020), which originated from two former European regional climate modelling projects, PRUDENCE (Christensen and Christensen, 2007) and ENSEMBLES (van der Linden and Mitchell, 2009).

Although RCMs have been shown to provide added value to the driving GCMs (Giorgi and Gutowski, 2015; Prein et al., 2016; Rummukainen, 2016; Giorgi, 2019; Iles et al., 2020), they may also lead to more noisy simulation results (e.g., Sørland et al., 2018). Despite the improved land-atmosphere coupling in RCMs, the representation of subsurface processes, i.e. groundwater dynamics and its coupling with the land surface and atmosphere, is generally oversimplified or neglected in existing RCMs. Commonly applied hydrology schemes in RCMs are typically based on 1D-parameterizations in the vertical direction with gravitational free drainage approach as the boundary condition at the bottom, and runoff generation at the land surface. Thus, while in RCMs there is generally no lateral subsurface flow in such a 1D-column parametrisation and often only the 1D-Richards' equation is solved (Niu et al., 2007; Campoy et al., 2013), some improvements have been made with respect

https://doi.org/10.5194/esd-2022-53
Preprint. Discussion started: 15 December 2022


Earth System Dynamics Discussions Open Access EGU

to more operational groundwater parameterizations (Schlemmer et al., 2018). Barlage et al. (2015), Keune et al. (2016) and Furusho-Percot et al. (2022) showed that the energy flux partitioning and, hence, near surface air temperatures are strongly influenced by groundwater, which also affects the representation of extreme heat events. In fact, many RCMs overestimate the frequency, duration, and intensity of heat waves (e.g., Vautard et al., 2013; Lhotka et al., 2018).

To study the evolution of future heat events in Europe, here we first investigate the evolution of past heat events over the European continent in a multi-model RCM ensemble driven by CMIP5 (Taylor et al., 2012) GCM control simulations. The RCM ensemble is complemented with a new dataset from the regional Terrestrial Systems Modelling Platform (TSMP), which allows for an integrated groundwater-to-atmosphere simulations, thus closing the terrestrial water cycle from bottom to top. We interrogate the statistics of the heat event characteristics (frequency, duration, intensity) to understand the impact of groundwater dynamics and potential consequences for climate change projections.

Section 2 introduces TSMP and its setup, describes the ensemble of the EURO-CORDEX climate change scenario RCM control runs, and the heat event analyses. In Sect. 3, we estimate the impact of groundwater on simulated heat events frequency, duration, and intensity, and assess TSMP's characteristics in simulating European heat events compared to the CORDEX ensemble. Section 4 provides summary and overall conclusions.

2 Methods

2.1 The Terrestrial Systems Modelling Platform (TSMP)

TSMP is a scale-consistent, highly modular, fully integrated soil-vegetation-atmosphere modelling system (e.g., Shrestha et al., 2014; Gasper et al., 2014). In the applied climate mode setup, TSMP consists of three component models: the atmospheric model COSMO (COnsortium for Small Scale Modelling) version 5.01 (Baldauf et al., 2011), the land surface model CLM (Community Land Model) version 3.5 (Oleson et al., 2004, 2008), and the hydrological model ParFlow version 3.2 (Kollet and Maxwell, 2006; Maxwell, 2013). The component models are externally coupled via the Ocean Atmosphere Sea Ice Soil (OASIS, version 3.0) Model Coupling Toolkit (MCT) coupler (Valcke, 2013), which passes states and fluxes between individual TSMP component models (for details see Shrestha et al., 2014; Gasper et al., 2014). In contrast to most RCMs, the TSMP closes the terrestrial water and energy cycles from the bedrock to the top of the atmosphere.

COSMO is a non-hydrostatic limited-area atmospheric model (e.g., Baldauf et al., 2011). The COSMO model is based on the primitive thermo-hydrodynamical Euler equations formulated in rotated geographical coordinates and generalized terrain-following height coordinates, describing compressible flow in a moist atmosphere. COSMO parameterization schemes are responsible for various physical processes, such as radiation, cloud microphysics, deep convection, etc. The lateral boundary conditions used for COSMO are usually provided by a coarse grid model, for instance, GCMs or reanalyses. In TSMP, the lower boundary conditions for COSMO (e.g., surface albedo, energy fluxes, surface temperature, surface humidity) are provided by the CLM land surface model via the component models coupling.

CLM is a biogeophysical model of the land surface (e.g., Oleson et al., 2004, 2008). It simulates land-atmosphere exchanges in response to atmospheric forcings. CLM consist of four components that describe biogeophysics, hydrologic cycle, biogeo-

https://doi.org/10.5194/esd-2022-53
Preprint. Discussion started: 15 December 2022


Earth System Dynamics Discussions Open Access EGU

chemistry and dynamic vegetation. In TSMP, CLM receives short-wave radiation, wind speeds, barometric pressure, precipitation, near-surface temperature and specific humidity from COSMO. CLM sends to ParFlow infiltration and evapotranspiration fluxes for each soil layer.

ParFlow is a hydrological model that simulates variably saturated three-dimensional subsurface hydrodynamics using Richards equation integrated with shallow overland flow based on a kinematic wave approximation (Ashby and Falgout, 1996; Maxwell and Miller, 2005; Kollet and Maxwell, 2006; Maxwell, 2013; Kuffour et al., 2020). ParFlow allows 3D-redistribution of subsurface water in a continuum approach. In TSMP, ParFlow replaces the hydrologic functionality of CLM.

2.2 TSMP setup

TSMP simulations were performed over Europe according to the EURO-CORDEX simulation protocol (e.g., Gutowski et al., 2016). The TSMP simulations were set up on the 0.11° CORDEX grid, i.e approximately 12.5 km. COSMO had a vertical range up to 22 km, CLM had a total depth of 3 m, while ParFlow reached a total depth of 57 m. COSMO contained 50 vertical levels, CLM had 10 soil layers that coincided with the upper ParFlow layers. ParFlow had a total of 15 layers with variable grid spacing increasing from top to bottom. The time step of ParFlow and CLM was 900 sec and 75 sec for COSMO. The coupling time step between the TSMP component models was 900 sec.

The TSMP climate change scenario control simulations were conducted for the historical time period from December 1949 to the end of 2005 constituting the first climate control simulation with a groundwater to top-of-atmosphere terrestrial model. Land surface, subsurface hydrology, and energy states were initialized with the moisture conditions of 1st of December 2011 from a spun-up evaluation run driven by ERA-Interim reanalysis (Furusho-Percot et al., 2019), which influenced the first years of the simulations and discarded in the analyses due to hydrodynamic spin-up. Forcing data and the lateral boundary conditions for the TSMP atmospheric component model were provided by the Max-Plank Institute's MPI-ESM-LR r1i1p1 GCM experiment, with a resolution of T63L47 (Giorgetta et al., 2013).

Detailed information on CLM and ParFLow specifications used in the TSMP setup has already been described earlier in Furusho-Percot et al. (2019); Hartick et al. (2021). In addition to these studies, we improved the subsurface geology using geological information from different databases as follows. We defined the soil texture in the top 10 layers of ParFlow from the Food and Agriculture Organization soil database (FAO, 1988). For the 5 lowest soil layers, we prescribed hydrogeology from the International Hydrogeological map of Europe (IHME) dataset (Duscher et al., 2015) and GLobal HYdrogeology MaPS (GLHYMPS) (Gleeson et al., 2014; Gleeson, 2018). As a proxy for alluvial aquifer systems in ParFlow, we used a pan-European River and Catchment Database (Vogt et al., 2007) with the assumption that alluvial aquifers lie underneath or in close proximity of existing rivers.

The TSMP output constitutes a dataset of all terrestrial essential climate variables at a 3-hourly time step.

2.3 The ensemble of EURO-CORDEX climate change scenario RCM control runs

The EURO-CORDEX ensemble of the multi-physics RCM climate change scenario control runs driven by different GCMs (r1i1p1 ensemble members) on 0.11° (EUR-11) grid is used in conjunction with the coupled TSMP modelling platform to

https://doi.org/10.5194/esd-2022-53
Preprint. Discussion started: 15 December 2022


Earth System Dynamics Discussions Open Access EGU

study the characteristics of summer heat events. All RCM ensemble members, with the exception of TSMP, include only a highly simplified representations of subsurface hydrodynamics. An overview of the RCM ensemble with 10 model products is provided in Table 1.

Table 1. Details on EURO-CORDEX RCM climate change scenario control runs used in the analysis.

Institution	RCM	GCM forcing data
FZJ	TSMP *(Shrestha et al., 2014)*	MPI-ESM-LR *(Mauritsen et al., 2019)*
CLMcom	CCLM4-8-17 *(Rockel et al., 2008)*	MPI-ESM-LR CNRM-CM5 *(Voldoire et al., 2013)*
CLMcom-ETH	COSMO-crCLIM *(e.g., Sørland et al., 2021)*	MPI-ESM-LR CNRM-CM5 NCC-NorESM1-M *(Bentsen et al., 2013)*
MPI-CSC	REMO2009 *(Jacob and Podzun, 1997)*	MPI-ESM-LR
GERICS	REMO2015 *(Pietikäinen et al., 2018)*	NCC-NorESM1-M NOAA-GFDL-ESM2G *(Dunne et al., 2012)* IPSL-CM5A-LR *(Dufresne et al., 2013)*

2.4 Heat event analyses

There is no generally accepted metric for heat events, and in particular for heat waves. While there is an emphasis on temperature-based diagnostics, current methods are often ambiguous or inconsistent, with a focus on certain impacts or sectors, describing heat events only partially (Perkins and Alexander, 2013). The most commonly used approach is built on the percentile temperature threshold (e.g., Zhang et al., 2005, 2011).

In this study, we define the start of a heat event as the first day with the mean daily temperature above the 90th percentile (e.g., Vautard et al., 2013). The 90th percentile is calculated for each grid point of the EURO-CORDEX domain for each day from a consecutive 5-day moving window centered on each calendar day of the 30-year reference period from 1961 to 1990. We assume that a day with the mean daily temperature exceeding the 90th percentile is a hot day (e.g., Sulikowska and Wypych, 2020), highlighted in dark red in Fig. 1. A series of hot days constitute a heat event. A heat event is interrupted if the mean daily temperature drops below the 90th percentile. The cumulative number of hot days during a heat event corresponds to the TG90p heat index, introduced by the European Climate Assessment and Dataset (ECA&D) project, complementing the core set of indices determined by the Expert Team on Climate Change Detection and Indices (ETCCDI) (e.g., Frich et al., 2002; Zhang et al., 2011). TG90p describes the number of days with

$$TG_{ij} > TG_{in}90, \tag{1}$$

where TG_{ij} is the mean daily temperature on day i of period j, and $TG_{in}90$ is the i-day 90th percentile of mean daily temperature calculated for a 5-day window centred on each calendar day of the 30-year reference period n.

https://doi.org/10.5194/esd-2022-53
Preprint. Discussion started: 15 December 2022

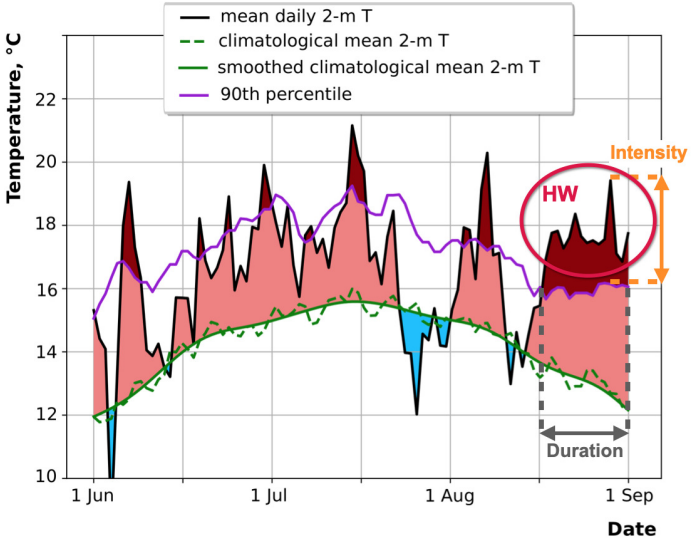

Heat event #	Start date	End date	Duration, days	Intensity, °C
1.	1.06	1.06	1	0,26
2.	6.06	9.06	4	2,71
3.	19.06	19.06	1	1,30
4.	24.06	24.06	1	1,07
5.	30.06	1.07	2	1,40
6.	7.07	7.08	2	0,41
7.	15.07	17.07	3	1,90
8.	3.08	4.08	2	0,63
9.	6.08	7.08	2	3,08
10.	17.08	31.08	15	3,28

Figure 1. Schematic of the methodology to detect a heat wave (HW) during the summer season. An example is given for June-July-August of 1972 for one grid point [250, 300] of the EURO-CORDEX domain. Data taken from the TSMP simulations. The solid black line is the mean daily 2-m air temperature in the summer of 1972. The dashed and solid green line represents the climatological raw average daily 2-m air temperature and Butterworth filtered data between 1961 to 1990, respectively. The solid violet line is the 90th percentile of the mean daily 2-m air temperature calculated from a 5-day window centered on each calendar day of the 1961-1990 reference period. The shaded light red colour indicates days with temperatures above the climatological mean, and the shaded dark red colour emphasizes days with temperatures above the 90th percentile, which we define as "hot days".

A heat event can be characterised by its duration, intensity, and frequency (e.g., Horton et al., 2016). A heat event duration is the number of consecutive days over which the heat event lasts. If a heat event lasts long enough, it can be classified as a heat wave. Similar to Fischer and Schär (2010), we define a heat wave as a spell of at least six consecutive days with mean daily temperatures above the local 90th percentile of the reference period (1961-1990). For explanation, Fig. 1 shows an example of a heat wave with the duration of 15 days. Note that the use of terms "heat event" and "heat wave" is similar in the context of this paper, with "heat event" referring to a series of unusually hot days. Furthermore, low-intensity heat events are also mentioned in literature as either a single-day or a multi-day event over a temperature threshold between the 85 and 92.5th percentile (Strathearn et al., 2022). In addition, some authors classify heat waves as low-intensity, severe, and extreme (Nairn and Fawcett, 2014).

In our analysis, a heat event intensity, HEI_m, is the maximum difference between the mean daily temperature and the calendar day 90th percentile within an individual heat event m (e.g., Vautard et al., 2013; Habeeb et al., 2015):

$$HEI_m = max(TG_{im} - TG_{in}90), \tag{2}$$

where TG_{im} is the mean daily temperature on day i during the heat event m. The intensity represents the severity of a heat event, see Fig. 1.

https://doi.org/10.5194/esd-2022-53
Preprint. Discussion started: 15 December 2022

Earth System Dynamics Discussions
Open Access
EGU

We define the frequency of heat events of a certain type, HEF_k, as the number of such heat events divided by the total number of heat events (e.g., Vautard et al., 2013):

$$HEF_k = \sum_{l=1}^{L} HE_{kl} / \sum_{j=1}^{J} HE_j, \tag{3}$$

where HE indicates a heat event, k denotes a specific feature of a heat event (e.g., heat events of a certain duration or intensity), l is the ordinal counter of a heat event of a certain type k within the total number L of heat events of this type, j is the ordinal counter of any heat event within the total number J of all heat events. For instance, from Fig. 1, the frequency of heat events with the duration of 2 days during the summer season is equal to the number of 2-day heat events (4 events) divided by the total number of all heat events (10 events). The resulting frequency is 0.4 and indicates that 40% of all heat events during the considered summer period have the duration of 2 days. Based on this definition, we estimate the frequency of hot days in summer as the number of hot days, or the TG90p index (33 days, see Fig. 1), divided by the total number of days in the summer season (92 days). The estimated frequency of hot days is approximately 0.36, indicating that 36% of all summer days are classified as hot days.

In this study, we examine past heat events in Europe during the summer season, evaluating their characteristics, such as frequency, duration, and intensity, based on the mean daily 2-m air temperatures on the native EURO-CORDEX EUR-11 grid in the ensemble of climate change scenario RCM control runs driven by different GCMs, as listed in Table 1. The analysis is performed for the summer season of the 30-year period 1976-2005, with regard to the reference period from 1961 to 1990 in each RCM. The analysis is adopted from the work of Vautard et al. (2013) and conducted over the arbitrarily chosen focus domain covering the European continent [10°W-30°E, 36°N-70°N] as shown in Fig. 2.

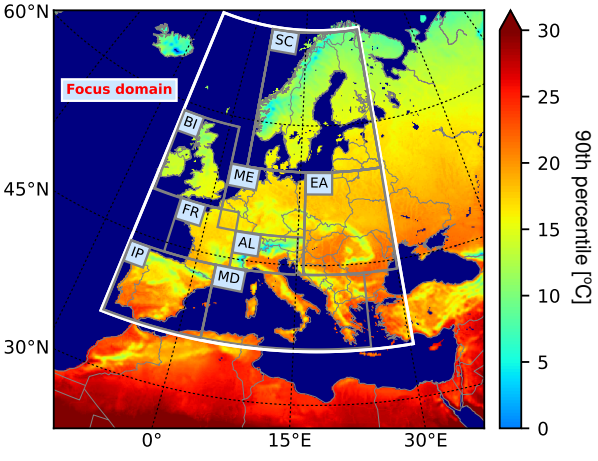

Figure 2. The 90th percentile of 2-m air temperatures averaged over the summer season simulated with TSM. The 90th percentile is obtained from a consecutive 5-day moving window centered on each calendar day of the summer season of the 30-year reference period from 1961 to 1990. The white border indicates the focus domain for the heat event analysis in our study [10°W-30°E, 36°N-70°N]. The smaller boxes with the respective abbreviations are the PRUDENCE regions: British Isles (BI), Iberian Peninsula (IP), France (FR), Mid-Europe (ME), Scandinavia (SC), Alps (AL), Mediterranean (MD) and Eastern Europe (EA).

https://doi.org/10.5194/esd-2022-53
Preprint. Discussion started: 15 December 2022

Earth System Dynamics
Discussions
Open Access
EGU

3 Results and Discussion

3.1 Influence of groundwater on the number of hot days in summer

We estimate the cumulative number of hot days, TG90p index, for each summer season during 1976-2005. The results from two regional climate models, the Terrestrial Systems Modelling Platform (TSMP) and CCLM (COSMO model in CLimate Mode; e.g., Rockel et al., 2008; Steger and Bucchignani, 2020), for several years are shown in Fig. 3 as an example. Both RCMs, TSMP and CCLM, are driven by the same forcing data from the Max-Plank Institute's MPI-ESM-LR r1i1p1 GCM experiment (e.g., Giorgetta et al., 2013). In addition, the TSMP atmospheric component model is CCLM compliant (see Sect. 2.1). The lower boundary condition for the TSMP atmospheric component model includes the groundwater feedback due to the coupling between the land surface component model CLM and the hydrologic component model ParFlow, unlike in the CCLM where

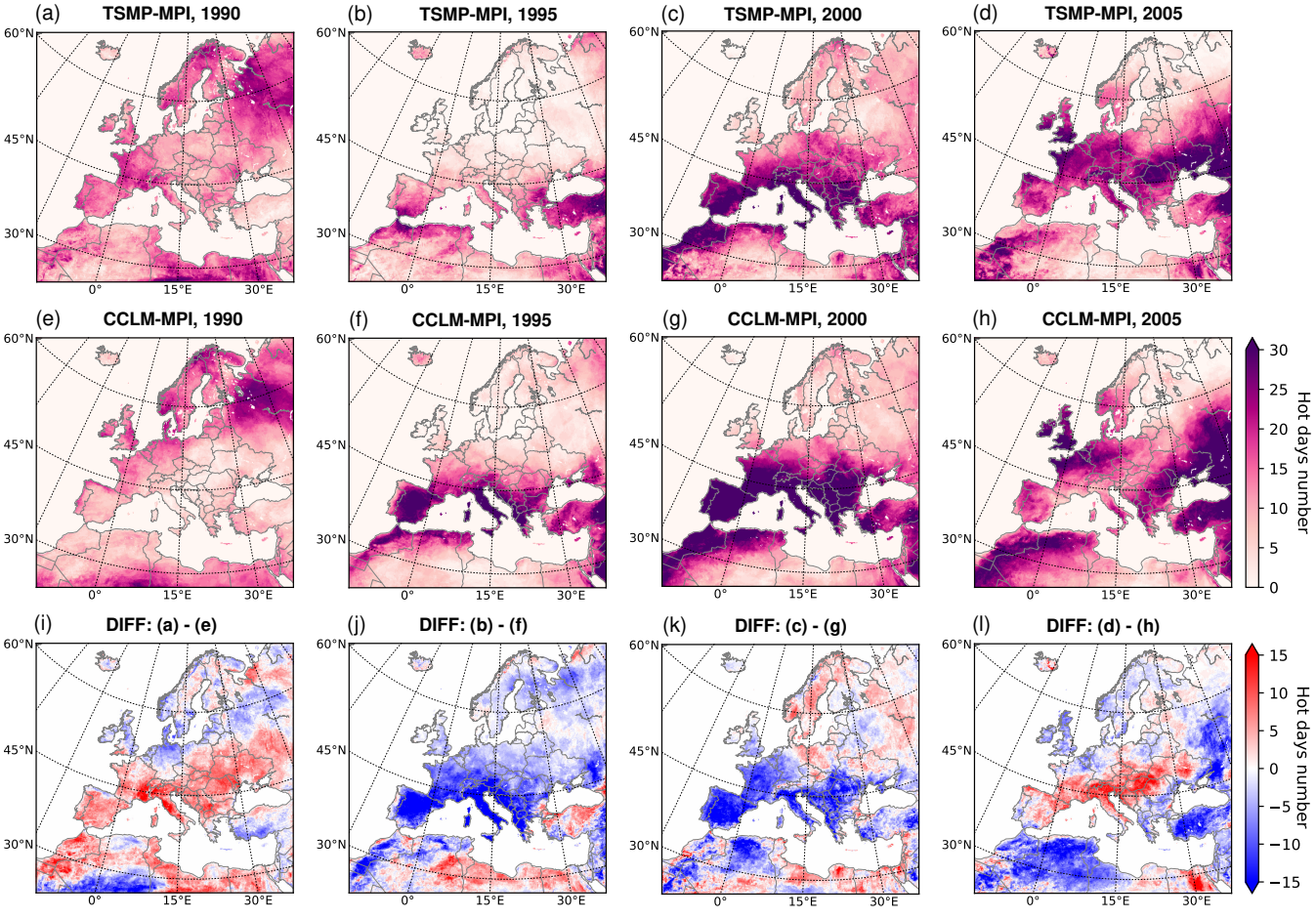

Figure 3. Cumulative number of hot days (TG90p index) during June-July-August. The example is shown for arbitrary selected years 1990, 1995, 2000, and 2005. The TG90p index is shown from the TSMP simulations (a, b, c, d) and CCLM simulations (e, f, g, h), their absolute differences are presented in (i,j, k, l).

https://doi.org/10.5194/esd-2022-53
Preprint. Discussion started: 15 December 2022

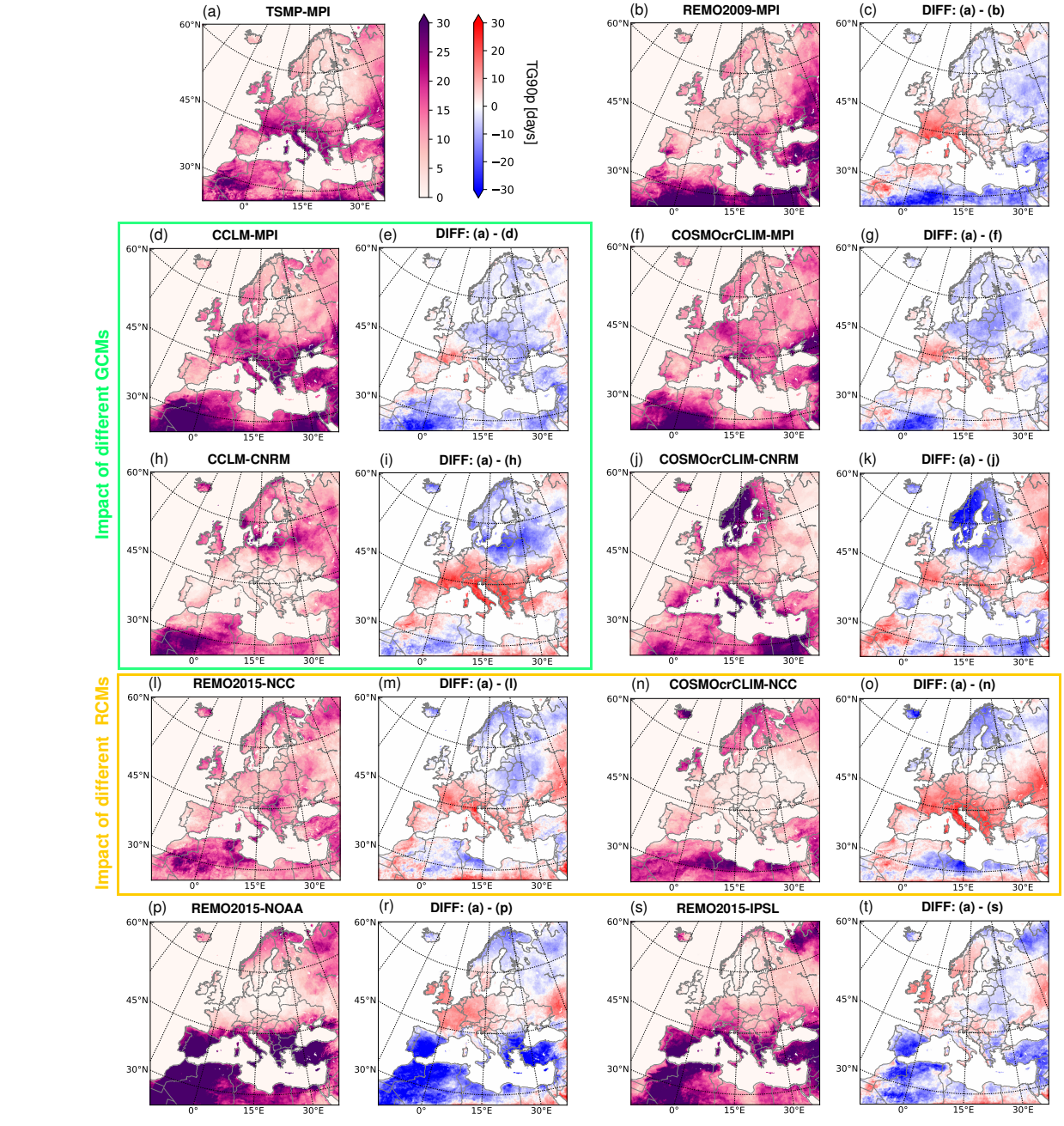

Figure 4. Cumulative number of hot days (TG90p index) during the summer season of 2003 for RCMs of the ensemble of EURO-CORDEX climate change scenario control runs (see Table 1), with respect to the reference period 1961-1990. The absolute differences in the TG90p index between TSMP and RCMs are also shown. Green and yellow boxes underline examples of different groups of ensemble member, e.g., different RCMs driven by the same GCMs, the same RCMs driven by different GCMs.

https://doi.org/10.5194/esd-2022-53
Preprint. Discussion started: 15 December 2022


Earth System Dynamics Discussions Open Access EGU

the soil processes are modelled with the TERRA-ML soil-vegetation land surface model. (e.g., Grasselt et al., 2008; Doms et al., 2013; Schulz et al., 2016).

There is good agreement in the overall pattern of the TG90p index calculated from TSMP and CCLM output. In 1990, with the exception of Northern Europe, TSMP shows larger TG90p values compared to CCLM (Fig. 3i). This year, the largest difference in the TG90p index between TSMP and CCLM is found in the Alps, reaching 15 days or more. Similar behaviour is observed also in 2005 with higher TG90p values in Central and Southern Europe in TSMP compared to CCLM (Fig. 3l). Unlike in 1990 and 2005, TSMP simulated fewer hot summer days than CCLM in 1995 and 2000, with a significant difference of more than 15 days in Central and Southern Europe (Fig. 3j, k). Thus, the impact of groundwater coupling apparently varies from year to year and also depends on the region under consideration. The effects of soil moisture memory can play an important role here by buffering droughts and weakening heat events. In contrast, past drought condition may be memorized in groundwater storage causing a delay in its recovery, and hence exacerbating the occurrence of heat events due to a reduction of latent heat and enhanced surface sensible heat flux (e.g., Erdenebat and Tomonori, 2018; Martínez-de la Torre and Miguez-Macho, 2019; Hartick et al., 2021).

The TG90p index for the EURO-CORDEX ensemble (see Table 1) for 2003 as an example is shown in Fig. 4. The considered ensemble members can be classified into three groups with respect to the used RCMs and GCMs forcing data: different RCMs driven by the same GCMs, the same RCMs driven by different GCMs, and different RCMs driven by different GCMs. The overall pattern of the TG90p index calculated from different RCMs driven by the same GCMs (Fig. 4a-g, h-k, l-o) agrees relatively well for 2003, although discrepancies in the exact magnitude and the spatial extent of TG90p are detectable. The differences of TG90p from the same RCMs driven by different GCMs (e.g., Fig. 4d, h or Fig. 4f, j, n) are comparable with the differences from different RCMs driven by the same GCMs. But in some cases the same RCM driven by different GCMs (Fig. 4l, p, s) has a significant difference in the TG90p index (e.g., 30 days or even more in the Iberian Peninsula), emphasizing a strong influence of the lateral boundary conditions from the different GCMs. Note that REMO2015, driven by NOAA and IPSL, imposes different distributions of the TG90p index (e.g., high values in the Iberian Peninsula) compared to the RCMs of the EURO-CORDEX ensemble, likely due to discrepancies in the large-scale atmospheric circulation in the driving GCMs. Furthermore, the TG90p differences shown in Fig. 4 highlight the different responses to groundwater coupling in the regions of energy-limited (Scandinavia and Northeastern Europe) and moisture-limited (Southern and Southeastern Europe) regimes.

3.2 Groundwater impact on the frequency of hot days

Due to connections of various factors other than groundwater coupling in the multi-model CORDEX ensemble (e.g., various model setups, conceptual and structural model uncertainties, different physical parameterizations, internal variability, representation of subsurface-land-atmosphere interactions, lower and lateral atmospheric GCM boundary conditions), it is challenging to reveal the exact cause and effect relationship of the explicit groundwater representation for simulated hot days and the associated heat events characteristics in RCMs. Moreover, the ensemble of EURO-CORDEX climate change scenario RCM control runs is not intended for direct comparison between individual models, as it includes different RCMs in combination

https://doi.org/10.5194/esd-2022-53
Preprint. Discussion started: 15 December 2022

Earth System Dynamics Discussions
Open Access
EGU

with different driving GCMs. However, as has been shown in previous studies, the consideration of an extended period, e.g., 30-years, allows to draw statistically conclusions.

In order to evaluate the impact of groundwater coupling on the interannual variability of hot summer days in RCMs, we examine the mean frequency of hot summer days in Europe in the ensemble of the EURO-CORDEX climate change scenario RCM control runs (see Table 1) from 1976 to 2005, with regard to the reference period 1961-1990 in each RCM (Fig. 5; see Sect. 2.4 for definitions). We calculate the mean frequency of hot summer days as the TG90p index, averaged over the total number of days during the summer season (92 days) and spatially averaged within all land-pixels of the focus domain (see Fig. 2). Comparison of the mean frequency of hot summer days from TSMP and individual RCMs, as well as the RCM multi-model mean, suggests that groundwater coupling does not seem to have a systematic impact on the occurrence of hot days. The interannual variability of summer heat events is strongly controlled by the large-scale atmospheric circulation imposed by the boundary conditions (see also Vautard et al., 2013). Thus the distribution of hot summer days largely depends on the driving GCMs.

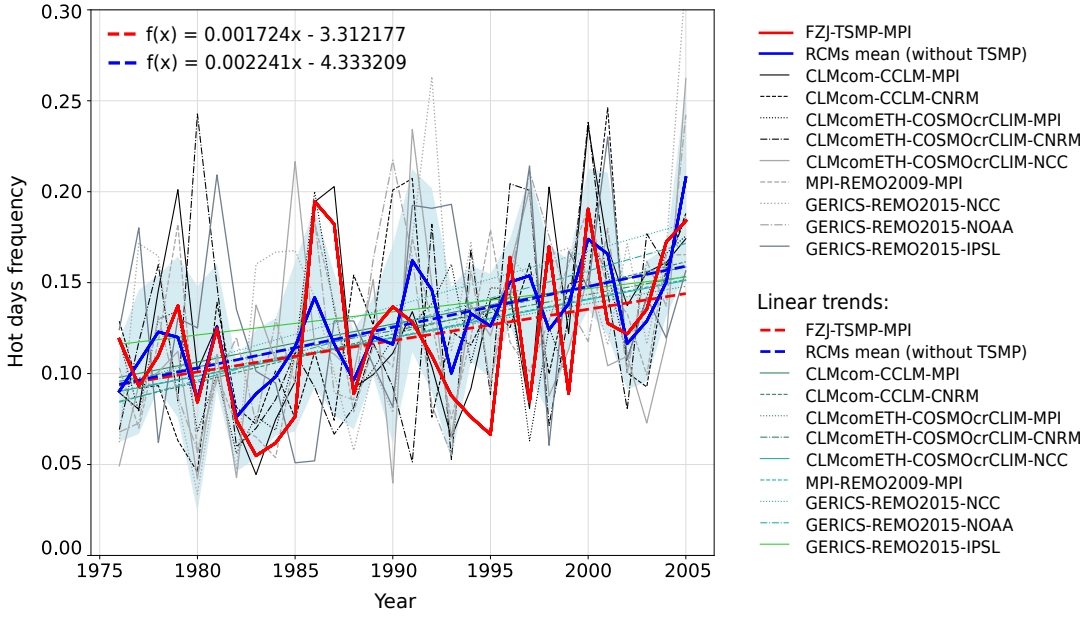

Figure 5. Time series of the mean frequency of hot summer days in Europe (averaged over the focus domain) and its linear trends during 1976-2005 with respect to the reference period 1961-1990, in the ensemble of EURO-CORDEX climate change scenario RCM control runs (see Table 1). The solid and dashed red lines show the mean frequency of hot days in summer from the TSMP simulation, as well as its linear trend. The black and grey lines represent the RCM ensemble frequencies of hot days, the shaded blue area represents their standard deviation, and the different green shaded lines are the linear trends of mean frequencies in each RCM respectively. The mean frequency of hot summer days, averaged over the multi-model RCM ensemble (excluding TSMP), is shown with the solid blue line, and its linear trend is shown with the dashed blue line.

https://doi.org/10.5194/esd-2022-53
Preprint. Discussion started: 15 December 2022

In Europe, an increasing linear trend of the frequency of hot summer days averaged over the focus domain is observed in all RCMs of the considered EURO-CORDEX ensemble (see Fig. 5). The frequency averaged over the multi-model RCM ensemble grows by about 1.5 times from 1976 to 2005 (dashed blue line in Fig. 5). The TSMP simulation gives the lowest linear trend of the frequency of hot summer days averaged over the focus domain in the considered EURO-CORDEX ensemble (dashed red line in Fig. 5). From the extrapolation functions shown in Fig. 5, the mean frequency of summer hot days in Europe is about 10% smaller in TSMP than in the RCM ensemble mean in 2005. Most RCMs in the considered EURO-CORDEX ensemble show an increasing linear trend also in individual PRUDENCE regions (Fig. A1). There are many studies that point to an increasing trend in the number of hot days worldwide: while the trend was not significant from 1950s until 1990s, it accelerates starting from 1990s and is associated with global warming (e.g., Frich et al., 2002; Perkins et al., 2012; Lhotka et al., 2018; Lorenz et al., 2019; Perkins-Kirkpatrick and Lewis, 2020).

3.3 Influence of groundwater on the occurrence of heat events of different duration

In this sub-section, we assess the impact of groundwater coupling on the duration of heat events in Europe. The annual number of heat events that occur on average per land grid point of the focus domain during the summer season between 1976 and 2005 as a function of the duration of these heat events is shown in Fig. 6a. The ratio of the number of heat events suggests

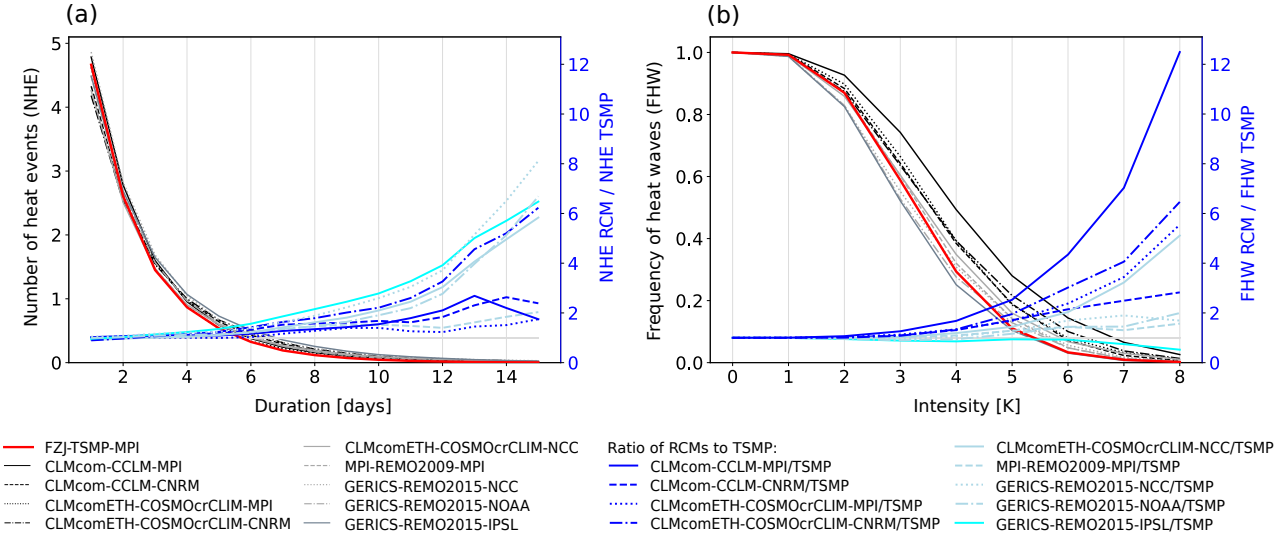

Figure 6. Average number of summer heat events (y-axis) of duration equal or larger than a given number of days (x-axis) as a function of this number of days (a); the averaging is performed over the total number of land-pixels of the focus domain (see Fig. 2) and the total number of years from 1976 to 2005 (30 years). Frequency of heat waves (y-axis) with an intensity higher or equal than a given value in abscissa occurring in the focus domain during the summer seasons, as a function of this intensity (b). The panels also show the ratio of quantities from RCMs to TSMP. Data are taken from the summer seasons between 1976 and 2005 with respect to the reference period 1961-1990 in each RCM of the ensemble of EURO-CORDEX climate change scenario control runs (see Table 1), represented with different colours and lines in the plots.

https://doi.org/10.5194/esd-2022-53
Preprint. Discussion started: 15 December 2022


Earth System Dynamics Discussions Open Access EGU

that groundwater coupling systematically impacts the duration of heat events in the simulations (presented with different types of blue lines in Fig. 6a). In TSMP, the mean number of heat events with a duration exceeding 2 days is systematically smaller compared to the RCMs of the considered EURO-CORDEX ensemble. In particular, the average number of heat waves (duration>6days), is 1.5-8 times lower. In addition, there is a small increase in the number of single-day heat events in TSMP compared to the CORDEX ensemble. Note that, for example,Vautard et al. (2013), Plavcová and Kyselý (2016) have previously found a systematic tendency of most RCMs to overestimate the number and duration of long heat waves in comparison to observations.

The lowest annual number of summer heat events per land-pixel within the PRUDENCE regions is found in Scandinavia, reaching about 3.9 heat events (Fig. A2). Compared to the RCMs of the considered EURO-CORDEX ensemble, TSMP systematically simulates fewer heat waves in all PRUDENCE regions except the British Isles. The strongest effect of groundwater coupling on buffering heat waves is observed in the Iberian Peninsula, France, and the Alps; heat waves with a duration >12 days occur even 10-20 times less often in TSMP compared to the CORDEX ensemble. Different responses to groundwater coupling in different PRUDENCE regions may be explained by the soil moisture-temperature feedback associated with the different evaporative regimes, energy-limited (predominant in Scandinavia and Northeastern Europe) versus moisture-limited (Southern and Southeastern Europe) (e.g., Koster et al., 2009; Knist et al., 2017; Haghighi et al., 2018; Jach et al., 2022).

3.4 Groundwater impact on the intensity of heat waves and the corresponding frequency

In this sub-section, we focus on heat waves, i.e. heat events with a duration exceeding 6 days. The dependency of the frequency of heat waves on their intensity is shown in Fig. 6b, see also Sect. 2.4 for definitions. The heat wave frequency presented in Fig. 6b describes the fraction of heat waves of a certain intensity that occurred during the 30-year summer periods from 1976 to 2005 in the focus domain in each RCM. The maximum frequency is equal to 1 for the intensity larger than 0 because all heat waves are taken into account for every RCM. From the ratio of heat wave frequencies of RCMs to TSMP (shown with different types of blue lines in Fig. 6b), we note a quite large spread of heat wave frequencies in the EURO-CORDEX ensemble, which increases towards heat waves of high intensity. TSMP exhibits a systematic behavior with fewer heat waves of high intensity compared to the CORDEX ensemble: the frequency of high-intensity heat waves is up to 12 times lower in TSMP. Our results also indicate that groundwater coupling has a stronger impact on the intensity of heat waves than on their duration in the TSMP simulations (see the ratio between CCLM-MPI and TSMP in Fig. 6a, b). Previously, Vautard et al. (2013) and Furusho-Percot et al. (2022) have shown that RCMs tend to overestimate the intensity of heat events, as well as the frequency of high-intensity heat waves.

The frequency of heat waves in different PRUDENCE regions has a different response to groundwater coupling in the simulations (Fig. A3). The response is almost negligible in Scandinavia, with good agreement between RCMs of the EURO-CORDEX ensemble, while it is significant in other PRUDENCE regions (e.g., Iberian Peninsula, France, Mid-Europe, Mediterranean, Eastern Europe) with a spread in the frequency of high-intensity heat waves of 20 times or more. The predominance of the energy-limited evaporative regime in Scandinavia and Northern Europe leads to a weaker land-atmosphere coupling, and thus to a relatively low impact of groundwater coupling on the frequency of simulated heat waves of high intensity.

https://doi.org/10.5194/esd-2022-53
Preprint. Discussion started: 15 December 2022


Earth System Dynamics Discussions
Open Access
EGU

4 Summary and Conclusions

We studied the impact of groundwater on summer heat events in a new dataset from a coupled regional climate system, the Terrestrial Systems Modelling Platform (TSMP), with an explicit representation of three-dimensional groundwater hydrodynamics, compared to an ensemble of EURO-CORDEX climate change scenario RCM control runs. In particular, we investigated the impact of groundwater coupling on the frequency of hot days, the occurrence of heat events of different duration, and the frequency of high-intensity heat waves in Europe between 1976 and 2005 with respect to the reference period 1961-1990.

Our results show that the impact of groundwater coupling on the frequency of hot days during the summer season, generally, depends on the time and region under consideration. There is an increasing trend in the frequency of hot summer days in Europe in all RCMs of the considered ensemble, whereas TSMP is the lowest. We found that the explicit representation of groundwater in RCMs leads to fewer simulated severe heat events. TSMP systematically shows a lower number of heat events lasting 6 or more days, so-called heat waves, on average in Europe; it is by about 1.5-8 times less than in the CORDEX ensemble. In addition, TSMP simulates a slightly higher number of single-day summer heat events compared to the CORDEX ensemble. The frequency of high-intensity heat waves is also lower in TSMP on average in Europe, up to 12 times, compared to the CODEX ensemble. The local impact of explicit groundwater representation in RCMs is linked to different evaporative regimes and, thus, regions with different strengths of land-atmosphere coupling. We found a smaller impact of groundwater coupling on the extreme heat event characteristics in regions with an energy-limited regime (e.g., British Isles and Scandinavia), and a stronger impact in regions with moisture-limited regime (Southern and Southeastern Europe), which is intuitive.

This study clearly indicates that a coupled regional climate system with a closed terrestrial water cycle, such as TSMP, systematically simulates a different climatology of extreme heat events compared to uncoupled RCMs of the EURO-CORDEX ensemble. The results emphasize the importance of groundwater coupling for simulating extreme heat events. Explicit representation of groundwater in RCMs may be a key for bias reduction in the occurrence of heat waves. In the future, this work will be extended to investigate regional climate projections and, in particular, the evolution of extreme heat events under different climate change scenarios in TSMP compared to uncoupled RCMs and their control simulations.

https://doi.org/10.5194/esd-2022-53
Preprint. Discussion started: 15 December 2022

Earth System Dynamics Discussions
Open Access
EGU

Appendix A: Impact of groundwater coupling on the heat events frequency, duration and intensity for PRUDENCE regions

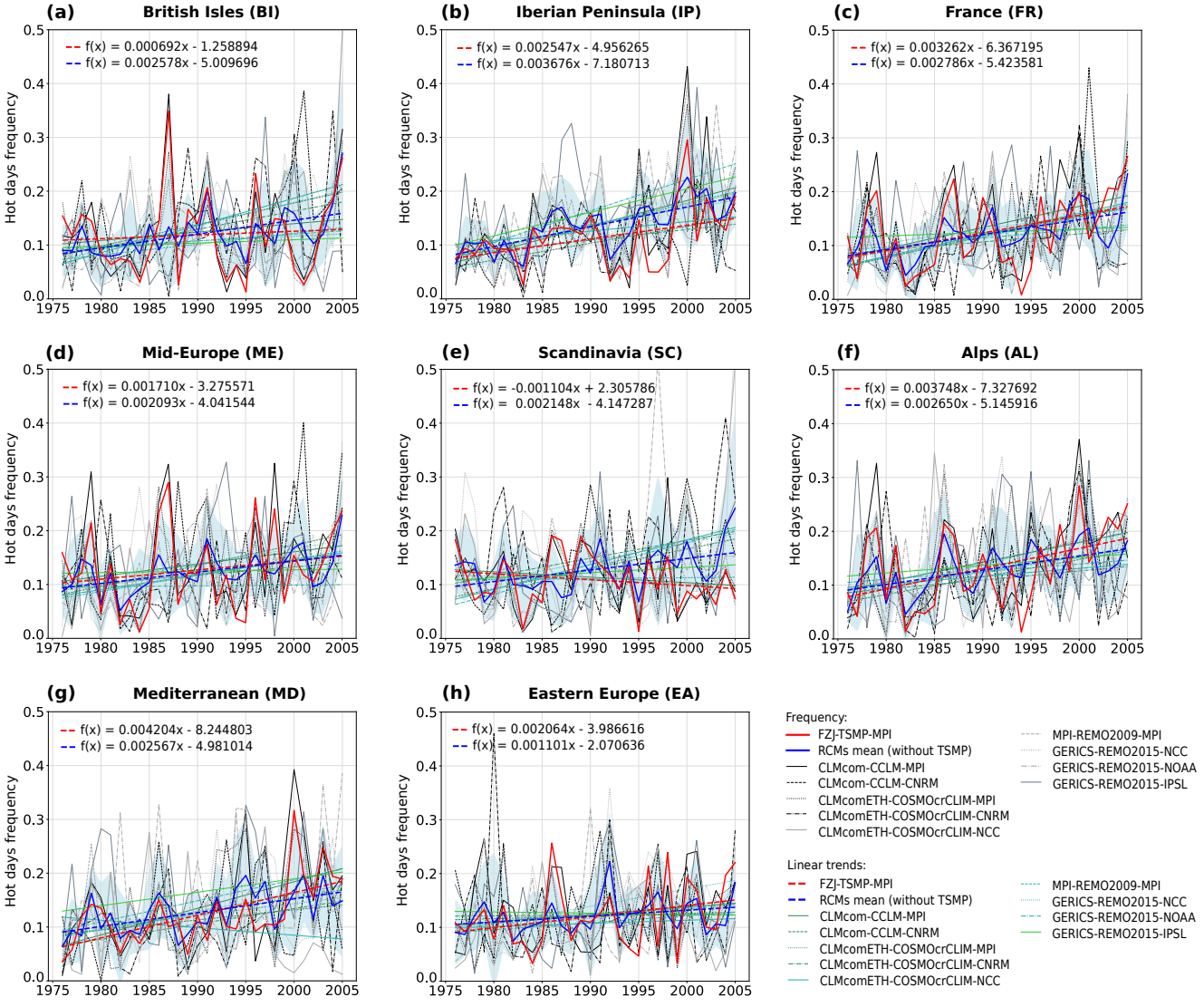

Figure A1. Time series of the mean frequency of hot summer days and its linear trends during 1976-2005 with respect to the reference period 1961-1990, in the ensemble of EURO-CORDEX climate change scenario RCM control runs (see Table 1) for PRUDENCE regions. Shown frequencies are calculated as the TG90p index, averaged over the total number of days during the summer season (92 days) and spatially averaged over all land-pixels in each PRUDENCE region. The solid and dashed red lines show the mean frequency of hot days in summer from TSMP simulation, as well as its linear trend. The black and grey lines represent the other RCMs' frequencies of hot days, the shaded blue area represents their standard deviation, and the different green tone lines are the linear trends. The mean frequency of hot summer days, averaged over the multi-model RCM ensemble (excluding TSMP), and its linear trend is shown with the solid and dashed blue lines.

https://doi.org/10.5194/esd-2022-53
Preprint. Discussion started: 15 December 2022

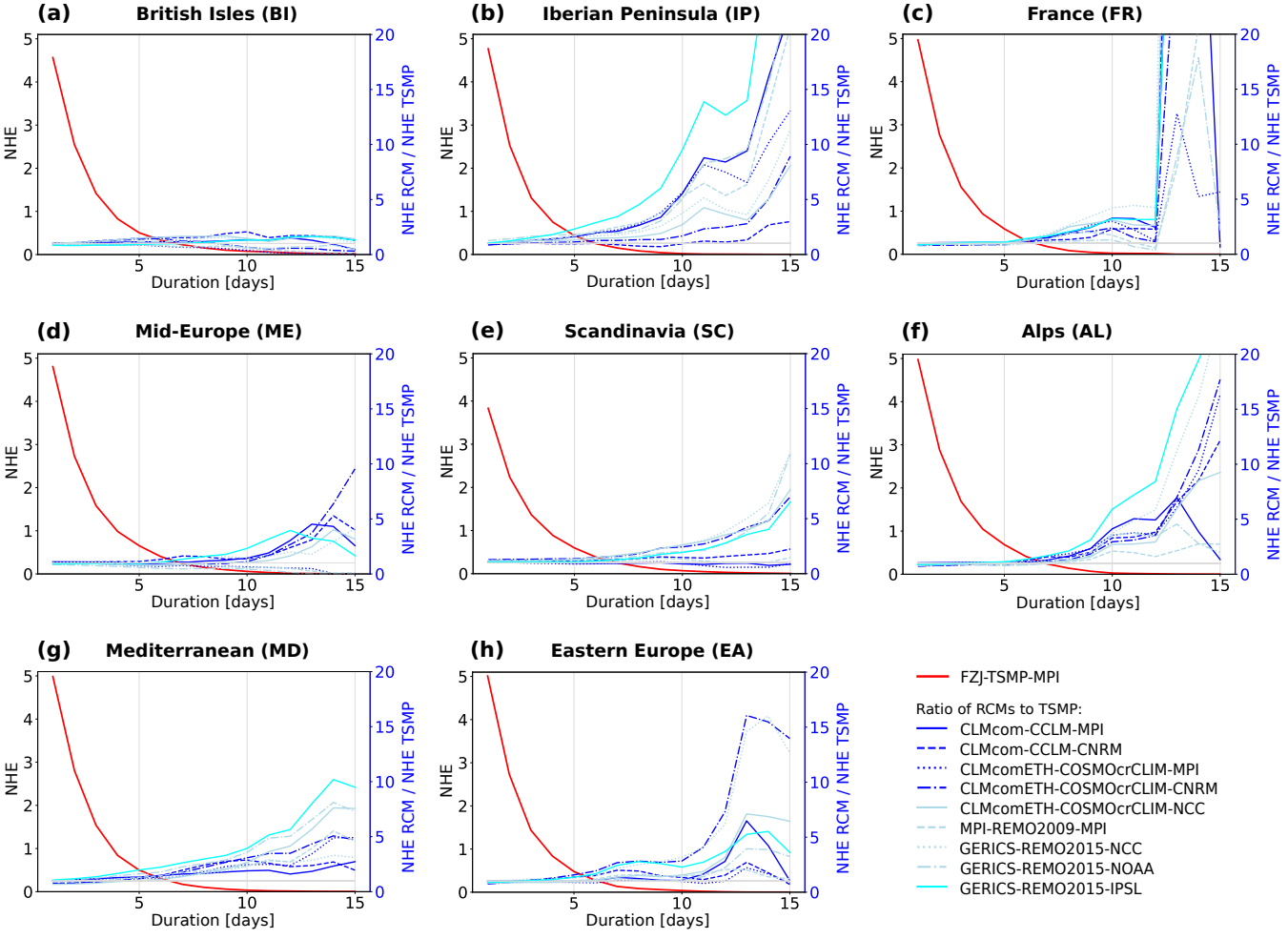

Figure A2. Average number of heat events (NHE) of duration equal to or larger than a given number of days (shown on X-axis) as a function of this number of days for PRUDENCE regions. The averaging is performed over the total number of land-pixels within every PRUDENCE region (see Fig. 2) and the total number of the investigated years from 1976 to 2005 (30 years). Solid red lines show the resulting average number of heat events from the TSMP simulations. To improve readability, the average number of heat events from RCMs is not shown on the sub-figures, instead we present the ratio of RCMs to TSMP with blue lines of different types. Data are taken from the summer season between 1976 and 2005 with respect to the reference period 1961-1990 in each RCM of the ensemble of EURO-CORDEX climate change scenario control runs (see Table 1).

https://doi.org/10.5194/esd-2022-53
Preprint. Discussion started: 15 December 2022

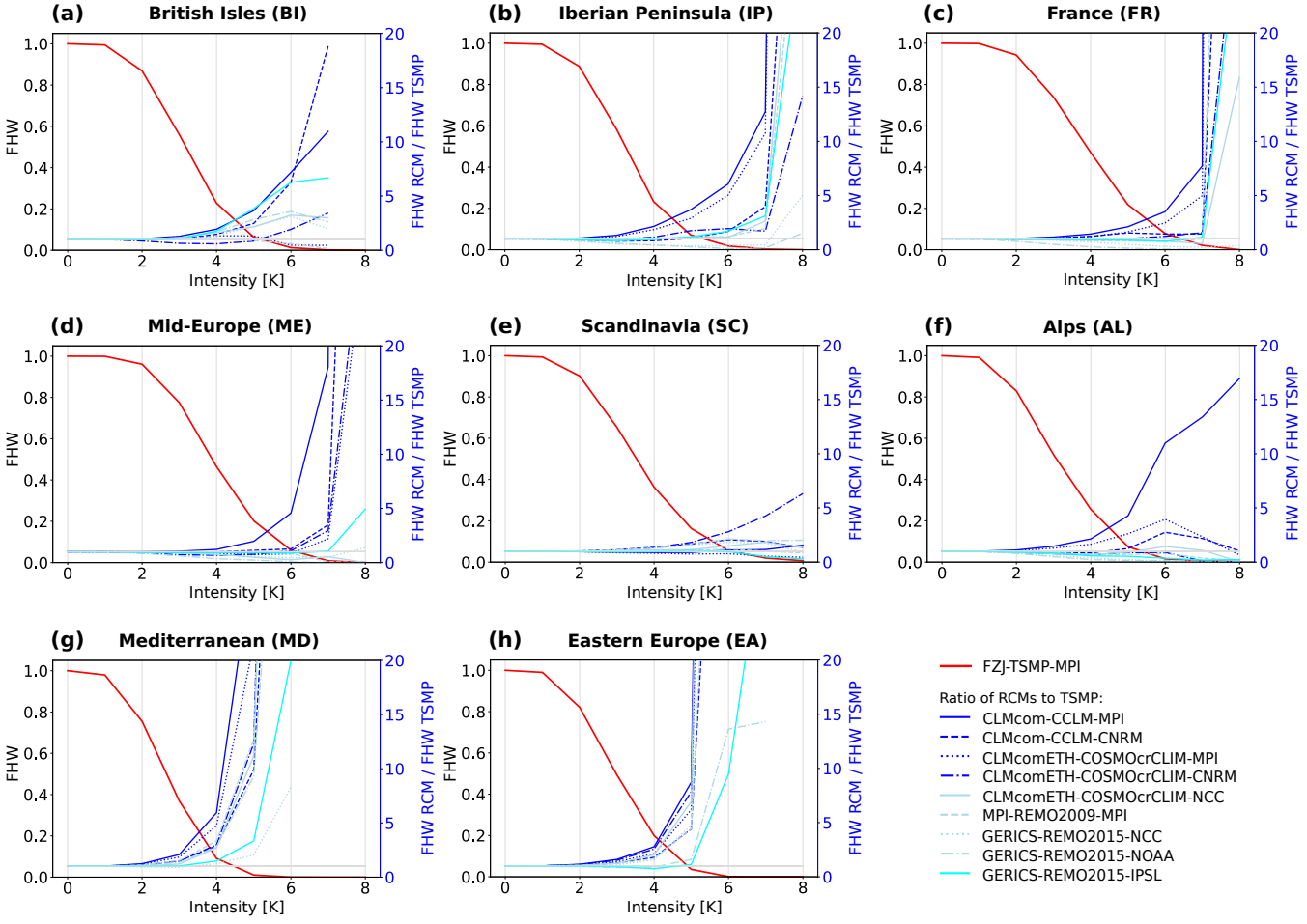

Figure A3. Frequency of heat waves (FHW) with an intensity equal to or greater than a given value in abscissa occurring in the PRUDENCE regions during the summer seasons between 1976 and 2005 as a function of this intensity. The intensity is calculated with respect to the reference period 1961-1990 in each RCM of the ensemble of EURO-CORDEX climate change scenario control runs (see Table 1). Solid red lines show the resulting frequency of heat waves from the TSMP simulations. To improve readability, the frequency of heat waves from RCMs is not shown on the sub-figures, instead we present the ratio of RCMs to TSMP with different blue lines. Note that in some PRUDENCE regions (a, g, h), the ratio of heat wave frequency of RCMs to TSMP ends before the range of abscissa because TSMP has zero values.

https://doi.org/10.5194/esd-2022-53
Preprint. Discussion started: 15 December 2022

Earth System Dynamics Discussions

Code and data availability. The TSMP v1.2.2 used in this work is available at the master GIT repository, https://github.com/HPSCTerrSys/TSMP. The dataset from the regional Terrestrial Systems Modeling Platform (TSMP) driven by MPI-ESM-LR r1i1p1 is currently available at https://datapub.fz-juelich.de/slts/regional_climate_tsmp_hi-cam/.

Author contributions. The study was designed by S.K. and K.G. with contributions by L.P-S. and N.W.. L.P.-S. conducted the model simulations and performed the data processing, N.W. provided technical and programming support. The analysis was conducted by L.P.-S. with further inputs from S.K. and K.G. L.P.-S. wrote the paper. All co-authors contributed to the interpretation of the results, active discussions, and revisions of the paper. The work was done under the supervision of S.K..

Competing interests. The authors declare that they have no conflict of interest.

Acknowledgements. This work was funded by the Helmholtz Association of German Research Centres (HGF) under the HI-CAM project (Helmholtz Initiative Climate Adaptation and Mitigation).We thank the EURO-CORDEX climate modelling groups for producing and making available their model output. We are grateful to the Max-Plank Institute for performing MPI-ESM-LR r1i1p1 GCM experiment and the German Climate Computing Centre (DKRZ) for providing the MPI-ESM-LR dataset. The authors gratefully acknowledge the Earth System Modelling Project (ESM) for funding this work by providing computing time on the ESM partition of the supercomputer JUWELS at the Jülich Supercomputing Centre (JSC) under the ESM project ID JIBG35. In addition, we thank the Simulation and Data Laboratory Terrestrial Systems of the Centre for High-Performance Scientific Computing in Terrestrial Systems (Geoverbund ABC/J, http://www.hpsc-terrsys.de) and the JSC for the computational support.

https://doi.org/10.5194/esd-2022-53
Preprint. Discussion started: 15 December 2022

References

Alexander, L. V., Zhang, X., Peterson, T. C., Caesar, J., Gleason, B., Klein Tank, A. M. G., Haylock, M., Collins, D., Trewin, B., Rahimzadeh, F., Tagipour, A., Rupa Kumar, K., Revadekar, J., Griffiths, G., Vincent, L., Stephenson, D. B., Burn, J., Aguilar, E., Brunet, M., Taylor, M., New, M., Zhai, P., Rusticucci, M., and Vazquez-Aguirre, J. L.: Global observed changes in daily climate extremes of temperature and precipitation, J. Geophys. Res. Atmos., 111, D05109, https://doi.org/10.1029/2005JD006290, 2006.

Amengual, A., Homar, V., Romero, R., Brooks, H., Ramis, C., Gordaliza, M., and Alonso, S.: Projections of heat waves with high impact on human health in Europe, Glob. Planet. Change, 119, 71–84, https://doi.org/10.1016/j.gloplacha.2014.05.006, 2014.

Ashby, S. F. and Falgout, R. D.: A Parallel Multigrid Preconditioned Conjugate Gradient Algorithm for Groundwater Flow Simulations, Nucl. Sci. Eng., 124, 145–159, https://doi.org/10.13182/NSE96-A24230, 1996.

Baldauf, M., Seifert, A., Förstner, J., Majewski, D., Raschendorfer, M., and Reinhardt, T.: Operational Convective-Scale Numerical Weather Prediction with the COSMO Model: Description and Sensitivities, Mon. Weather Rev., 139, 3887–3905, https://doi.org/10.1175/MWR-D-10-05013.1, 2011.

Barlage, M., Tewari, M., Chen, F., Miguez-Macho, G., Yang, Z.-L., and Niu, G.-Y.: The effect of groundwater interaction in North American regional climate simulations with WRF/Noah-MP, Clim. Change, 129, 485–498, https://doi.org/10.1007/s10584-014-1308-8, 2015.

Barriopedro, D., Fischer, E. M., Luterbacher, J., Trigo, R. M., and R., G.-H.: The Hot Summer of 2010: Redrawing the Temperature Record Map of Europe, Science, 332, 220–224, https://doi.org/10.1126/science.1201224, 2011.

Bentsen, M., Bethke, I., Debernard, J. B., Iversen, T., Kirkevåg, A., Seland, Ø., Drange, H., Roelandt, C., Seierstad, I. A., Hoose, C., and Kristjánsson, J. E.: The Norwegian Earth System Model, NorESM1-M – Part 1: Description and basic evaluation of the physical climate, Geosci. Model Dev., 6, 687–720, https://doi.org/10.5194/gmd-6-687-2013, 2013.

Bosello, F., Roson, R., and Tol, R.: Economy-wide Estimates of the Implications of Climate Change: Sea Level Rise, Environ. Resource Econ., 37, 549–571, https://doi.org/10.1007/s10640-006-9048-5, 2007.

Campoy, A., Ducharne, A., Cheruy, F., Hourdin, F., Polcher, J., and Dupont, J. C.: Response of land surface fluxes and precipitation to different soil bottom hydrological conditions in a general circulation model, J. Geophys. Res. Atmos., 118, 10 725–10 739, https://doi.org/10.1002/jgrd.50627, 2013.

Christensen, J. H. and Christensen, O. B.: A summary of the PRUDENCE model projections of changes in European climate by the end of this century, Clim. Change, 81, 7–30, https://doi.org/10.1007/s10584-006-9210-7, 2007.

Christidis, N., Jones, G., and Stott, P.: Dramatically increasing chance of extremely hot summers since the 2003 European heatwave, Nature Clim. Change, 5, 46–50, https://doi.org/10.1038/nclimate2468, 2015.

Ciscar, J.-C., Iglesias, A., Feyen, L., Szabó, L., Van Regemorter, D., Amelung, B., Nicholls, R., Watkiss, P., Christensen, O. B., Dankers, R., Garrote, L., Goodess, C. M., Hunt, A., Moreno, A., Richards, J., and Soria, A.: Physical and economic consequences of climate change in Europe, Proc. Natl. Acad. Sci., 108, 2678–2683, https://doi.org/10.1073/pnas.1011612108, 2011.

Dirmeyer, P. A., Balsamo, G., Blyth, E. M., Morrison, R., and Cooper, H. M.: Land-Atmosphere Interactions Exacerbated the Drought and Heatwave Over Northern Europe During Summer 2018, AGU Advances, 2, e2020AV000283, https://doi.org/10.1029/2020AV000283, 2021.

Doms, G., Föorstner, J., Heise, E., Herzog, H.-J., Mironov, D., Raschendorfer, M., Reinhardt, T., Ritter, B., Schrodin, R., Schulz, J.-P., and Vogel, G.: Consortium for small-scale modelling: A description of the nonhydrostatic regional COSMO model. Part II: Physical parameterization, Tech. rep., https://doi.org/10.5676/DWD_pub/nwv/cosmo-doc_5.00_II, 2013.

https://doi.org/10.5194/esd-2022-53
Preprint. Discussion started: 15 December 2022

Dufresne, J.-L., Foujols, M.-A., Denvil, S., and et al.: Climate change projections using the IPSL-CM5 Earth System Model: from CMIP3 to CMIP5, Clim. Dyn., 40, 2123–2165, https://doi.org/10.1007/s00382-012-1636-1, 2013.

Dunne, J. P., John, J. G., Adcroft, A. J., Griffies, S. M., Hallberg, R. W., Shevliakova, E., Stouffer, R. J., Cooke, W., Dunne, K. A., Harrison, M. J., Krasting, J. P., Malyshev, S. L., Milly, P. C. D., Phillipps, P. J., Sentman, L. T., Samuels, B. L., Spelman, M. J., Winton, M., Wittenberg, A. T., and Zadeh, N.: GFDL's ESM2 Global Coupled Climate–Carbon Earth System Models. Part I: Physical Formulation and Baseline Simulation Characteristics, J. Clim., 25, 6646–6665, https://doi.org/10.1175/JCLI-D-11-00560.1, 2012.

Duscher, K., Günther, A., Richts, A., Clos, P., Philipp, U., and Struckmeier, W.: The GIS layers of the "International Hydrogeological Map of Europe 1:1,500,000" in a vector format, Hydrogeol. J., 23, 1867–1875, https://doi.org/10.1007/s10040-015-1296-4, 2015.

Erdenebat, E. and Tomonori, S.: Role of soil moisture-atmosphere feedback during high temperature events in 2002 over Northeast Eurasia, Prog. Earth. Planet. Sci., 5, 37, https://doi.org/10.1186/s40645-018-0195-4, 2018.

FAO: FAO/UNESCO Soil Map of the World, Revised Legend, with corrections and updates, World Soil Resources Report 60, FAO, Rome, https://www.fao.org/3/bl892e/bl892e.pdf, 1988.

Fischer, E. M. and Schär, C.: Consistent geographical patterns of changes in high-impact European heatwaves, Nat. Geosci., 3, 398–403, https://doi.org/10.1038/ngeo866, 2010.

Fischer, E. M., Seneviratne, S. I., Lüthi, D., and Schär, C.: Contribution of land-atmosphere coupling to recent European summer heat waves, Geophys. Res. Lett., 34, L06707, https://doi.org/10.1029/2006GL029068, 2007.

Frich, P., Alexander, L. V., Della-Marta, P., Gleason, B., Haylock, M., Klein Tank, A. M. G., and Peterson, T.: Observed coherent changes in climatic extremes during the second half of the twentieth century, Clim. Res., 19, 193–212, https://doi.org/10.3354/cr019193, 2002.

Furusho-Percot, C., Goergen, K., Hartick, C., Kulkarni, K., Keune, J., and Kollet, S.: Pan-European groundwater to atmosphere terrestrial systems climatology from a physically consistent simulation, Sci. Data, 6, 320, https://doi.org/10.1038/s41597-019-0328-7, 2019.

Furusho-Percot, C., Goergen, K., Hartick, C., Poshyvailo-Strube, L., and Kollet, S.: Groundwater Model Impacts Multiannual Simulations of Heat Waves, Geophys. Res. Lett., 49, e2021GL096781, https://doi.org/10.1029/2021GL096781, 2022.

Gasper, F., Goergen, K., Shrestha, P., Sulis, M., Rihani, J., Geimer, M., and Kollet, S.: Implementation and scaling of the fully coupled Terrestrial Systems Modeling Platform (TerrSysMP v1.0) in a massively parallel supercomputing environment – a case study on JUQUEEN (IBM Blue Gene/Q), Geosci. Model Dev., 7, 2531–2543, https://doi.org/10.5194/gmd-7-2531-2014, 2014.

Giorgetta, M. A., Jungclaus, J., Reick, C. H., Legutke, S., Bader, J., Böttinger, M., Brovkin, V., Crueger, T., Esch, M., Fieg, K., Glushak, K., Gayler, V., Haak, H., Hollweg, H.-D., Ilyina, T., Kinne, S., Kornblueh, L., Matei, D., Mauritsen, T., Mikolajewicz, U., Mueller, W., Notz, D., Pithan, F., Raddatz, T., Rast, S., Redler, R., Roeckner, E., Schmidt, H., Schnur, R., Segschneider, J., Six, K. D., Stockhause, M., Timmreck, C., Wegner, J., Widmann, H., Wieners, K.-H., Claussen, M., Marotzke, J., and Stevens, B.: Climate and carbon cycle changes from 1850 to 2100 in MPI-ESM simulations for the Coupled Model Intercomparison Project phase 5, J. Adv. Model. Earth Syst., 5, 572–597, https://doi.org/10.1002/jame.20038, 2013.

Giorgi, F.: Thirty Years of Regional Climate Modeling: Where Are We and Where Are We Going next?, J. Geophys. Res. Atmos., 124, 5696–5723, https://doi.org/10.1029/2018JD030094, 2019.

Giorgi, F. and Gutowski, W. J.: Regional Dynamical Downscaling and the CORDEX Initiative, Annu. Rev. Environ. Resour., 40, 467–490, https://doi.org/10.1146/annurev-environ-102014-021217, 2015.

Gleeson, T.: GLobal HYdrogeology MaPS (GLHYMPS) of permeability and porosity, Borealis, V1, https://doi.org/10.5683/SP2/DLGXYO, 2018.

https://doi.org/10.5194/esd-2022-53
Preprint. Discussion started: 15 December 2022

Gleeson, T., Moosdorf, N., Hartmann, J., and van Beek, L. P. H.: A glimpse beneath earth's surface: GLobal HYdrogeology MaPS (GLHYMPS) of permeability and porosity, Geophys. Res. Lett., 41, 3891–3898, https://doi.org/10.1002/2014GL059856, 2014.

Grasselt, René and Schüttemeyer, D., Warrach-Sagi, K., Ament, F., and Simmer, C.: Validation of TERRA-ML with discharge measurements, Meteorol. Z., 17, 763–773, https://doi.org/10.1127/0941-2948/2008/0334, 2008.

Gutowski, W. J., Giorgi, F., Timbal, B., Frigon, A., Jacob, D., Kang, H.-S., Raghavan, K., Lee, B., Lennard, C., Nikulin, G., O'Rourke, E., Rixen, M., Solman, S., Stephenson, T., and Tangang, F.: WCRP COordinated Regional Downscaling EXperiment (CORDEX): a diagnostic MIP for CMIP6, Geosci. Model Dev., 9, 4087–4095, https://doi.org/10.5194/gmd-9-4087-2016, 2016.

Gutowski, W. J., Ullrich, P. A., Hall, A., Leung, L. R., O'Brien, T. A., Patricola, C. M., Arritt, R. W., Bukovsky, M. S., Calvin, K. V., Feng, Z., Jones, A. D., Kooperman, G. J., Monier, E., Pritchard, M. S., Pryor, S. C., Qian, Y., Rhoades, A. M., Roberts, A. F., Sakaguchi, K., Urban, N., and Zarzycki, C.: The Ongoing Need for High-Resolution Regional Climate Models: Process Understanding and Stakeholder Information, Bull. Am. Meteorol. Soc., 101, E664–E683, https://doi.org/10.1175/BAMS-D-19-0113.1, 2020.

Habeeb, D., Vargo, J., and Stone, B.: Rising heat wave trends in large US cities, Nat. Hazards, 76, 1651–1665, https://doi.org/10.1007/s11069-014-1563-z, 2015.

Haghighi, E., Short Gianotti, D. J., Akbar, R., Salvucci, G. D., and Entekhabi, D.: Soil and Atmospheric Controls on the Land Surface Energy Balance: A Generalized Framework for Distinguishing Moisture-Limited and Energy-Limited Evaporation Regimes, Water Resour. Res., 54, 1831–1851, https://doi.org/https://doi.org/10.1002/2017WR021729, 2018.

Hari, V., Rakovec, O., Markonis, Y., Hanel, M., and Kumar, R.: Increased future occurrences of the exceptional 2018-2019 Central European drought under global warming, Sci. Rep., 10, 12207, https://doi.org/10.1038/s41598-020-68872-9, 2020.

Hartick, C., Furusho-Percot, C., Goergen, K., and Kollet, S.: An Interannual Probabilistic Assessment of Subsurface Water Storage Over Europe Using a Fully Coupled Terrestrial Model, Water Resour. Res., 57, e2020WR027828, https://doi.org/https://doi.org/10.1029/2020WR027828, 2021.

Horton, R. M., Mankin, J. S., Lesk, C., Coffel, E., and Raymond, C.: Review of Recent Advances in Research on Extreme Heat Events, Curr. Clim. Change. Rep., 2, 242–259, https://doi.org/10.1007/s40641-016-0042-x, 2016.

Iles, C. E., Vautard, R., Strachan, J., Joussaume, S., Eggen, B. R., and Hewitt, C. D.: The benefits of increasing resolution in global and regional climate simulations for European climate extremes, Geosci. Model Dev., 13, 5583–5607, https://doi.org/10.5194/gmd-13-5583-2020, 2020.

Ionita, M., Nagavciuc, V., Kumar, R., and Rakovec, O.: On the curious case of the recent decade, mid-spring precipitation deficit in central Europe, NPJ Clim. Atmos. Sci., 3, 49, https://doi.org/10.1038/s41612-020-00153-8, 2020.

Jach, L., Schwitalla, T., Branch, O., Warrach-Sagi, K., and Wulfmeyer, V.: Sensitivity of land–atmosphere coupling strength to changing atmospheric temperature and moisture over Europe, Earth Syst. Dynam., 13, 109–132, https://doi.org/10.5194/esd-13-109-2022, 2022.

Jacob, D. and Podzun, R.: Sensitivity studies with the regional climate model REMO, Meteorl. Atmos. Phys., 63, 119–129, https://doi.org/10.1007/BF01025368, 1997.

Jacob, D., Teichmann, C., Sobolowski, S., and et al.: Regional climate downscaling over Europe: perspectives from the EURO-CORDEX community, Reg. Environ. Change, 20, 51, https://doi.org/10.1007/s10113-020-01606-9, 2020.

Keune, J., Gasper, F., Goergen, K., Hense, A., Shrestha, P., Sulis, M., and Kollet, S.: Studying the influence of groundwater representations on land surface-atmosphere feedbacks during the European heat wave in 2003, J. Geophys. Res. Atmos., 121, 13 301–13 325, https://doi.org/10.1002/2016JD025426, 2016.

https://doi.org/10.5194/esd-2022-53
Preprint. Discussion started: 15 December 2022

Knist, S., Goergen, K., Buonomo, E., Christensen, O. B., Colette, A., Cardoso, R. M., Fealy, R., Fernández, J., García-Díez, M., Jacob, D., Kartsios, S., Katragkou, E., Keuler, K., Mayer, S., van Meijgaard, E., Nikulin, G., Soares, P. M. M., Sobolowski, S., Szepszo, G., Teichmann, C., Vautard, R., Warrach-Sagi, K., Wulfmeyer, V., and Simmer, C.: Land-atmosphere coupling in EURO-CORDEX evaluation experiments, J. Geophys. Res. Atmos., 122, 79–103, https://doi.org/10.1002/2016JD025476, 2017.

Kollet, S. J. and Maxwell, R. M.: Integrated surface–groundwater flow modeling: A free-surface overland flow boundary condition in a parallel groundwater flow model, Adv. Water. Resour., 29, 945–958, https://doi.org/10.1016/j.advwatres.2005.08.006, 2006.

Koster, R. D., Schubert, S. D., and Suarez, M. J.: Analyzing the Concurrence of Meteorological Droughts and Warm Periods, with Implications for the Determination of Evaporative Regime, J. Clim., 22, 3331–3341, https://doi.org/10.1175/2008JCLI2718.1, 2009.

Kuffour, B. N. O., Engdahl, N. B., Woodward, C. S., Condon, L. E., Kollet, S., and Maxwell, R. M.: Simulating coupled surface–subsurface flows with ParFlow v3.5.0: capabilities, applications, and ongoing development of an open-source, massively parallel, integrated hydrologic model, Geosci. Model Dev., 13, 1373–1397, https://doi.org/10.5194/gmd-13-1373-2020, 2020.

Lhotka, O. and Kyselý, J.: Characterizing joint effects of spatial extent, temperature magnitude and duration of heat waves and cold spells over Central Europe, Int. J. Climatol., 35, 1232–1244, https://doi.org/10.1002/joc.4050, 2015.

Lhotka, O., Kyselý, J., and Plavcová, E.: Evaluation of major heat waves' mechanisms in EURO-CORDEX RCMs over Central Europe, Clim. Dyn., 50, 4249–4262, https://doi.org/10.1007/s00382-017-3873-9, 2018.

Liu, X., He, B., Guo, L., Huang, L., and Chen, D.: Similarities and Differences in the Mechanisms Causing the European Summer Heatwaves in 2003, 2010, and 2018, Earth's Future, 8, e2019EF001386, https://doi.org/10.1029/2019EF001386, 2020.

Lorenz, R., Stalhandske, Z., and Fischer, E. M.: Detection of a Climate Change Signal in Extreme Heat, Heat Stress, and Cold in Europe From Observations, Geophys. Res. Lett., 46, 8363–8374, https://doi.org/10.1029/2019GL082062, 2019.

Martínez-de la Torre, A. and Miguez-Macho, G.: Groundwater influence on soil moisture memory and land–atmosphere fluxes in the Iberian Peninsula, Hydrol. Earth Syst. Sci., 23, 4909–4932, https://doi.org/10.5194/hess-23-4909-2019, 2019.

Masson-Delmotte, V., Zhai, P., Pirani, A., Connors, S., Péan, C., Berger, S., Caud, N.and Chen, Y., Goldfarb, L., Gomis, M., Huang, M., Leitzell, K., Lonnoy, I., Matthews, J., Maycock, T., Waterfield, T., Yelekçi, O., Yu, R., and B., Z., eds.: IPCC report, Climate Change 2021: The Physical Science Basis. Contribution of Working Group I to the Sixth Assessment Report of the Intergovernmental Panel on Climate Change, Cambridge University Press, Cambridge, United Kingdom and New York, NY, USA, https://www.ipcc.ch/report/ar6/wg1/downloads/report/IPCC_AR6_WGI_FullReport.pdf, 2021.

Mauritsen, T., Bader, J., Becker, T., and et al.: Developments in the MPI-M Earth System Model version 1.2 (MPI-ESM1.2) and Its Response to Increasing CO2, J. Adv. Model. Earth Syst., 11, 998–1038, https://doi.org/10.1029/2018MS001400, 2019.

Maxwell, R. M.: A terrain-following grid transform and preconditioner for parallel, large-scale, integrated hydrologic modeling, Adv. Water. Resour., 53, 109–117, https://doi.org/10.1016/j.advwatres.2012.10.001, 2013.

Maxwell, R. M. and Miller, N. L.: Development of a Coupled Land Surface and Groundwater Model, J. Hydrometeorol., 6, 233–247, https://doi.org/10.1175/JHM422.1, 2005.

Mearns, L. O., Lettenmaier, D. P., and McGinnis, S.: Uses of Results of Regional Climate Model Experiments for Impacts and Adaptation Studies: the Example of NARCCAP, Curr. Clim. Change Rep., 1, 1–9, https://doi.org/10.1007/s40641-015-0004-8, 2015.

Miralles, D. G., van den Berg, M. J., Teuling, A. J., and de Jeu, R. A. M.: Soil moisture-temperature coupling: A multiscale observational analysis, Geophys. Res. Lett., 39, L21707, https://doi.org/10.1029/2012GL053703, 2012.

Molina, M. O., Sánchez, E., and Gutiérrez, C.: Future heat waves over the Mediterranean from an Euro-CORDEX regional climate model ensemble, Sci. Rep., 10, 8801, https://doi.org/10.1038/s41598-020-65663-0, 2020.

https://doi.org/10.5194/esd-2022-53
Preprint. Discussion started: 15 December 2022

Mu, M., De Kauwe, M. G., Ukkola, A. M., Pitman, A. J., Guo, W., Hobeichi, S., and Briggs, P. R.: Exploring how groundwater buffers the influence of heatwaves on vegetation function during multi-year droughts, Earth Syst. Dyn., 12, 919–938, https://doi.org/10.5194/esd-12-919-2021, 2021.

Myhre, G., Alterskjær, K., Stjern, C. W., Hodnebrog, Ø., Marelle, L., Samset, B. H., Sillmann, J., Schaller, N., Fischer, E., Schulz, M., and Stohl, A.: Frequency of extreme precipitation increases extensively with event rareness under global warming, Sci. Rep., 9, 16063, https://doi.org/10.1038/s41598-019-52277-4, 2019.

Nairn, J. R. and Fawcett, R. J. B.: The excess heat factor: a metric for heatwave intensity and its use in classifying heatwave severity, Int. J. Environ. Res. Public Health, 12, 227–253, https://doi.org/10.3390/ijerph120100227, 2014.

Naumann, G., Cammalleri, C., Mentaschi, L., and Feyen, L.: Increased economic drought impacts in Europe with anthropogenic warming, Nat Clim Chang, 11, 485–491, https://doi.org/10.1038/s41558-021-01044-3, 2021.

Niu, G.-Y., Yang, Z.-L., Dickinson, R. E., Gulden, L. E., and Su, H.: Development of a simple groundwater model for use in climate models and evaluation with Gravity Recovery and Climate Experiment data, J. Geophys. Res. Atmos., 112, D07103, https://doi.org/10.1029/2006JD007522, 2007.

Oleson, K., Dai, Y., Bonan, G. B., Bosilovichm, M., Dickinson, R., Dirmeyer, P., and et al.: Technical Description of the Community Land Model (CLM) (No. NCAR/TN-461+STR), Tech. rep., University Corporation for Atmospheric Research, https://doi.org/10.5065/D6N877R0, 2004.

Oleson, K. W., Niu, G.-Y., Yang, Z.-L., Lawrence, D. M., Thornton, P. E., Lawrence, P. J., Stöckli, R., Dickinson, R. E., Bonan, G. B., Levis, S., Dai, A., and Qian, T.: Improvements to the Community Land Model and their impact on the hydrological cycle, J. Geophys. Res. Biogeosci., 113, G01021, https://doi.org/10.1029/2007JG000563, 2008.

Perkins, S. E. and Alexander, L. V.: On the Measurement of Heat Waves, J. Clim., 26, 4500–4517, https://doi.org/10.1175/JCLI-D-12-00383.1, 2013.

Perkins, S. E., Alexander, L. V., and Nairn, J. R.: Increasing frequency, intensity and duration of observed global heatwaves and warm spells, Geophys. Res. Lett., 39, L20714, https://doi.org/10.1029/2012GL053361, 2012.

Perkins-Kirkpatrick, S. E. and Lewis, S. C.: Increasing trends in regional heatwaves, Nat. Commun., 11, 3357, https://doi.org/10.1038/s41467-020-16970-7, 2020.

Pietikäinen, J.-P., Markkanen, T., Sieck, K., Jacob, D., Korhonen, J., Räisänen, P., Gao, Y., Ahola, J., Korhonen, H., Laaksonen, A., and Kaurola, J.: The regional climate model REMO (v2015) coupled with the 1-D freshwater lake model FLake (v1): Fenno-Scandinavian climate and lakes, Geosci. Model Dev., 11, 1321–1342, https://doi.org/10.5194/gmd-11-1321-2018, 2018.

Plavcová, E. and Kyselý, J.: Overly persistent circulation in climate models contributes to overestimated frequency and duration of heat waves and cold spells, Clim. Dyn., 46, 2805–2820, https://doi.org/10.1007/s00382-015-2733-8, 2016.

Prein, A. F., Gobiet, A., Truhetz, H., Keuler, K., Goergen, K., Teichmann, C., Fox Maule, C., van Meijgaard, E., Déqué, M., Nikulin, G., Vautard, R., Colette, A., Kjellström, E., and Jacob, D.: Precipitation in the EURO-CORDEX 0.11° and 0.44° simulations: high resolution, high benefits?, Clim. Dyn., 46, 383–412, https://doi.org/10.1007/s00382-015-2589-y, 2016.

Rockel, B., Will, A., and Hense, A.: The Regional Climate Model COSMO-CLM (CCLM), Meteorol. Z., 17, 347–348, https://doi.org/10.1127/0941-2948/2008/0309, 2008.

Rummukainen, M.: Added value in regional climate modeling, WIREs Clim. Change, 7, 145–159, https://doi.org/10.1002/wcc.378, 2016.

Russo, S., Sillmann, J., and Fischer, E. M.: Top ten European heatwaves since 1950 and their occurrence in the coming decades, Environ. Res. Lett., 10, 124003, https://doi.org/10.1088/1748-9326/10/12/124003, 2015.

https://doi.org/10.5194/esd-2022-53
Preprint. Discussion started: 15 December 2022

Schlemmer, L., Schär, C., Lüthi, D., and Strebel, L.: A Groundwater and Runoff Formulation for Weather and Climate Models, J. Adv. Model. Earth Syst., 10, 1809–1832, https://doi.org/10.1029/2017MS001260, 2018.

Schulz, J.-P., Vogel, G., Becker, C., Kothe, S., Rummel, U., and Ahrens, B.: Evaluation of the ground heat flux simulated by a multi-layer land surface scheme using high-quality observations at grass land and bare soil, Meteorol. Z., 25, 607–620, https://doi.org/10.1127/metz/2016/0537, 2016.

Shrestha, P., Sulis, M., Masbou, M., Kollet, S., and Simmer, C.: A Scale-Consistent Terrestrial Systems Modeling Platform Based on COSMO, CLM, and ParFlow, Mon. Weather Rev., 142, 3466–3483, https://doi.org/10.1175/MWR-D-14-00029.1, 2014.

Song, Y. M., Wang, Z. F., Qi, L. L., and Huang, A. N.: Soil Moisture Memory and Its Effect on the Surface Water and Heat Fluxes on Seasonal and Interannual Time Scales, J. Geophys. Res. Atmos., 124, 10 730–10 741, https://doi.org/10.1029/2019JD030893, 2019.

Sørland, S. L., Schär, C., Lüthi, D., and Kjellström, E.: Bias patterns and climate change signals in GCM-RCM model chains, Environ. Res. Lett., 13, 074017, https://doi.org/10.1088/1748-9326/aacc77, 2018.

Sørland, S. L., Brogli, R., Pothapakula, P. K., Russo, E., Van de Walle, J., Ahrens, B., Anders, I., Bucchignani, E., Davin, E. L., Demory, M.-E., Dosio, A., Feldmann, H., Früh, B., Geyer, B., Keuler, K., Lee, D., Li, D., van Lipzig, N. P. M., Min, S.-K., Panitz, H.-J., Rockel, B., Schär, C., Steger, C., and Thiery, W.: COSMO-CLM regional climate simulations in the Coordinated Regional Climate Downscaling Experiment (CORDEX) framework: a review, Geosci. Model Dev., 14, 5125–5154, https://doi.org/10.5194/gmd-14-5125-2021, 2021.

Stegehuis, A. I., Vogel, M. M., Vautard, R., Ciais, P., Teuling, A. J., and Seneviratne, S. I.: Early Summer Soil Moisture Contribution to Western European Summer Warming, J. Geophys. Res. Atmos., 126, e2021JD034646, https://doi.org/10.1029/2021JD034646, 2021.

Steger, C. and Bucchignani, E.: Regional Climate Modelling with COSMO-CLM: History and Perspectives, Atmosphere, 11, 1250, https://doi.org/10.3390/atmos11111250, 2020.

Stott, P. A., Stone, D. A., and Allen, M. R.: Human contribution to the European heatwave of 2003, Nature, 432, 610–614, https://doi.org/10.1038/nature03089, 2004.

Strathearn, M., Osborne, N. J., and Selvey, L. A.: Impact of low-intensity heat events on mortality and morbidity in regions with hot, humid summers: a scoping literature review, Int. J. Biometeorol., 66, 1013–1029, https://doi.org/10.1007/s00484-022-02243-z, 2022.

Sulikowska, A. and Wypych, A.: Summer temperature extremes in Europe: how does the definition affect the results?, Theor. Appl. Climatol., 141, 19–30, https://doi.org/10.1007/s00704-020-03166-8, 2020.

Taylor, K. E., Stouffer, R. J., and Meehl, G. A.: An Overview of CMIP5 and the Experiment Design, Bull. Am. Meteorol. Soc., 93, 485–498, https://doi.org/10.1175/BAMS-D-11-00094.1, 2012.

Tomczyk, A. M. and Bednorz, E.: Heat waves in Central Europe and their circulation conditions, Int. J. Climatol., 36, 770–782, https://doi.org/10.1002/joc.4381, 2016.

Valcke, S.: The OASIS3 coupler: a European climate modelling community software, Geosci. Model Dev., 6, 373–388, https://doi.org/10.5194/gmd-6-373-2013, 2013.

van der Linden, P. and Mitchell, J. F. B.: ENSEMBLES: Climate Change and Its Impacts – Summary of Research and Results from the ENSEMBLES Project, Met Office Hadley Centre, FitzRoy Road, Exeter EX1 3PB, UK, http://ensembles-eu.metoffice.com/docs/Ensembles_final_report_Nov09.pdf, 2009.

Vautard, R., Yiou, P., D'Andrea, F., de Noblet, N., Viovy, N., Cassou, C., Polcher, J., Ciais, P., Kageyama, M., and Fan, Y.: Summertime European heat and drought waves induced by wintertime Mediterranean rainfall deficit, Geophys. Res. Lett., 34, L07711, https://doi.org/10.1029/2006GL028001, 2007.

https://doi.org/10.5194/esd-2022-53
Preprint. Discussion started: 15 December 2022

Vautard, R., Gobiet, A., Jacob, D., and et al.: The simulation of European heat waves from an ensemble of regional climate models within the EURO-CORDEX project, Clim. Dyn., 41, 2555–2575, https://doi.org/10.1007/s00382-013-1714-z, 2013.

Vogt, J., Soille, P., De Jager, A., Rimaviciute, E., Mehl, W., Foisneau, S., Bodis, K., Dusart, J., Paracchini, M., Haastrup, P., and Bamps, C.: A pan-European River and Catchment Database, JRC Reference Report, Joint Research Centre, Institute for Environment and Sustainability, https://doi.org/10.2788/35907, 2007.

Voldoire, A., Sanchez-Gomez, E., Salas y Mélia, D., and et al: The CNRM-CM5.1 global climate model: description and basic evaluation, Clim. Dyn., 40, 2091–2121, https://doi.org/10.1007/s00382-011-1259-y, 2013.

Zhang, R., Sun, C., Zhu, J., Zhang, R., and Li, W.: Increased European heat waves in recent decades in response to shrinking Arctic sea ice and Eurasian snow cover, NPJ Clim. Atmos. Sci., 3, 7, https://doi.org/10.1038/s41612-020-0110-8, 2020.

Zhang, X., Hegerl, G., Zwiers, F., and Kenyon, J.: Avoiding Inhomogeneity in Percentile-Based Indices of Temperature Extremes, J. Clim., 38, 1641–1651, https://doi.org/10.1175/JCLI3366.1, 2005.

Zhang, X., Alexander, L., Hegerl, G. C., Jones, P., Tank, A. K., Peterson, T. C., Trewin, B., and Zwiers, F. W.: Indices for monitoring changes in extremes based on daily temperature and precipitation data, WIREs Clim. Change, 2, 851–870, https://doi.org/10.1002/wcc.147, 2011.